Available on CMS information server

CMS NOTE AN-2006/101

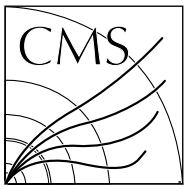

The Compact Muon Solenoid Experiment

CMS Note

Mailing address: CMS CERN, CH-1211 GENEVA 23, Switzerland

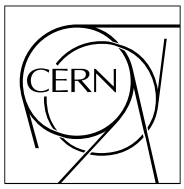

October 17, 2006

Reconstruction of V0s and photon conversions with the pixel detector

Ferenc Siklér

KFKI Research Institute for Particle and Nuclear Physics, Budapest, Hungary

Abstract

Although neutral particles do not create hits in the pixel detector, they can be observed via their charged daughters. The combination of helices of secondaries enables the reconstruction of low p_T weakly-decaying particles (K^0_S, Λ and $\overline{\Lambda}$) decaying before the first pixel barrel. Low p_T photons converting in the beam-pipe or in the first pixel barrel are detectable as well.

Table 1: Some important parameters of neutral particles examined in this note: mass m, decay length, charged decay mode, branching ratio and decay momentum q.

Particle	m [GeV/c^2]	Length [cm]	Daughters	Branching	q [GeV/c]
K^0_S	0.4976	$c\tau$ = 2.68	$\pi^+\pi^-$	68.9%	0.209
Λ	1.1157	$c\tau$ = 7.89	$p\pi^-$	63.9%	0.101
γ	0	$9/7X_0$	e^+e^-	100%	small

1 Introduction

The reconstruction and identification of neutral particles is important for hadron physics where the measured particle yields, spectra and correlations have to be compared to model predictions [1]. The physics of rare high p_T events also needs good knowledge about the characteristics of the underlying background collisions. It is important for high energy physics in general.

Silicon detectors can detect charged particles with good position and momentum resolution. Some weakly-decaying neutral particles, such as K^0_S, Λ and $\overline{\Lambda}$, have sizeable probability to decay far from the primary vertex of the event. This way their reconstruction is less difficult than that of resonances decaying very close to the primary vertex. The long-lived neutral particles can be reconstructed via their charged decay mode (see Table 1).

At the same time silicon detectors can be used to reconstruct photons with help of their conversion to e^+e^- pairs in the material of the beam-pipe, silicon detector and support. The probability of conversion is $x/(9/7X_0)$, where x is the thickness of the material, X_0 is its radiation length. For 0.1 cm material this amounts to 0.22% in beryllium and 0.83% in silicon. While the physics process is quite different, photon conversions in all other aspects are very similar to decays and they will be treated together.

In the CMS detector the high occupancy of silicon strips in central A+A collisions makes their inclusion into V0 finding difficult. The use of silicon pixels alone allows to use the same analysis for low multiplicity p+p, p+A and high multiplicity A+A events. At the same time this choice enables the reconstruction of very low p_T particles, even down to 0.1 GeV/c for pions, with low fake rate [2]. The analysis presented here uses charged particles reconstructed from pixel hit triplets only. It means that only those neutrals can be found which decay not farther than the first pixel barrel layer (Fig. 1). Sizeable fraction of produced neutrals satisfies this condition. The probability that a particle decays within a radius r is

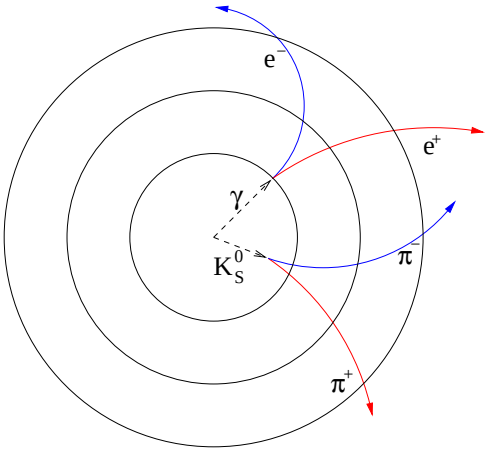

Figure 1: Schematic view of a V0 decay and a photon conversion. The pixel barrels are given by the black circles.

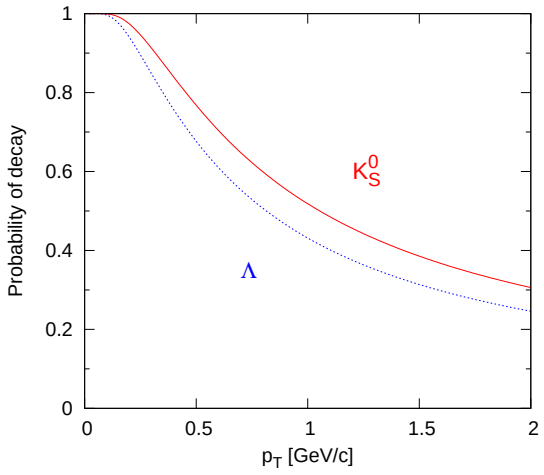

Figure 2: Probability of decay before the first pixel barrel layer ($r \approx 4$ cm) as function of p_T of the particle. Curves for K^0_S (solid red) and Λ (dashed blue) are given.

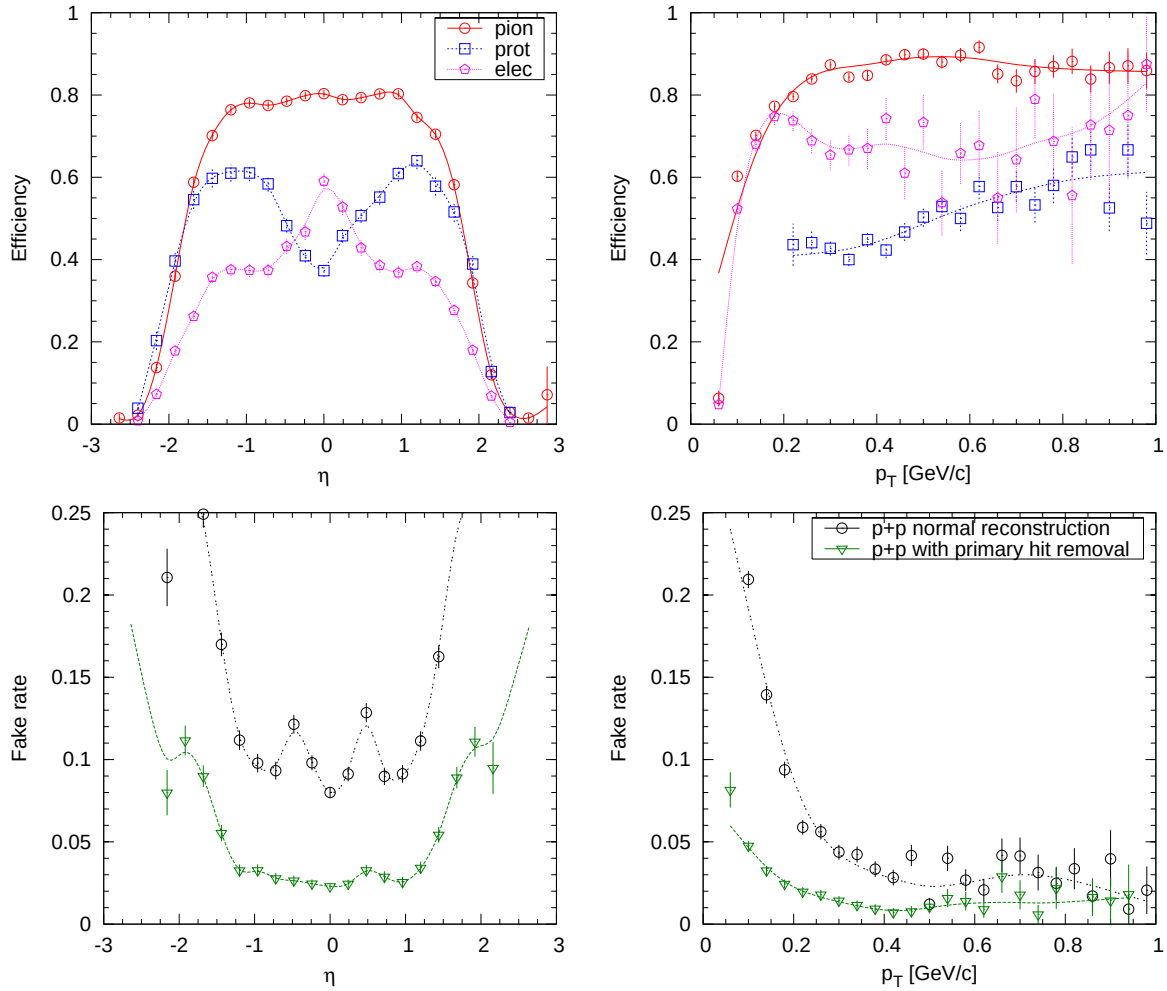

Figure 3: Efficiency (top) and fake rate (bottom) of secondary particle reconstruction as a function of η (left) and as a function of p_T (right, if the particle is in the range $|\eta| < 1$). A charged particle was taken to be secondary if it is was created farther than 0.2 cm from the beam-line. Efficiency values for pions, protons and electrons are given separately (top). The fake rate is shown for normal reconstruction and with the removal of hits belonging to primary tracks (bottom).

$$P(r) = 1 - \exp\left(-\frac{r}{c\tau}\frac{m}{p_T}\right) \tag{1}$$

which is independent of pseudo-rapidity η. The result of the calculation with $r = 4$ cm as function of p_T is shown in Fig. 2. About every second K^0_S and Λ decays even a $p_T = 1$ GeV/c.

1.1 Secondary particles

These studies are based on 25 000 single minimum bias p+p events (Pythia generator), reconstructed with modified hit triplet finding [2] using the standard settings (`originHalfLength` = 15 cm; `originZPos` = 0 cm), but much wider cylinder of origin (`originRadius` = 3.0 cm) and much lower minimal p_T (`ptMin` = 0.075 GeV/c). The efficiency and fake rate of secondary particle reconstruction as a function of η and p_T is shown in Fig. 3. Lines in the plots are drawn to guide the eye.

The fake rate of secondary particles, and the background of the V0 finding, can be reduced. Most of the produced particles are primaries which can be well reconstructed by a narrow cylinder of origin (`originRadius` = 0.2 cm). Those reconstructed hits which belong to primary tracks are removed next. In a second turn, secondary particles are searched using the remaining hits with a wider setting (`originRadius` = 3.0 cm). The fake rate of secondaries is significantly reduced (Fig. 3 bottom). This improvement enables V0 finding in p+p events with pile-up and in high multiplicity Pb+Pb collisions as well. At the same time the drawback of the idea is that it also removes most

Table 2: Important parameters which can be used for cleaning the V0 candidates. The cut ranges used in the analysis are given as well.

Notation	Meaning	Cut [cm]
b_{pos}	impact parameter of the positive daughter	$>$0.2
b_{neg}	impact parameter of the negative daughter	$>$0.2
Δr	distance of the projected circles of the daughters	$<$0.2
Δz	distance of closest points of the projected circles in z	$<$0.2
r or d	distance of the vertex from the beam-line or primary vertex	$>$0.5
b	impact parameter of the mother wrt the beam-line or primary vertex	$<$0.2

of the protons coming from Λ and $\overline{\Lambda}$ decays (see Section 2.1).

It was shown that fake rate strongly depends on the luminosity and the single event multiplicity (see [2]). If the hit removal is applied to events with different amount of pile-up, the higher luminosity events will loose more possibly valid hits due to their higher fake content. This is reflected in the smaller reconstruction efficiency of V0s and photon conversions (Section 3.3).

2 V0 finding

In the small volume of the pixel detector the magnetic field is practically constant, the charged particles propagate on helices. The search for V0 candidates reduces to the determination of the closest point of two helices. The description of a fast method can be found in the Appendix A. It calculates the following parameters:

- distance Δr of the projected circles
- distance Δz of the closest points in z direction
- the position of the pair of the closest points V_1 and V_2
- momenta $\vec{p_1}$ and $\vec{p_2}$ of the tracks at V_1 and V_2

The decay point or production vertex $\vec{r}$ is the midpoint of the line segment V_1V_2. The momentum vector $\vec{p}$ and the impact parameter b of the neutral mother particle are given by

$$\vec{p} = \vec{p_1} + \vec{p_2} \qquad\qquad b = \left| \vec{r} - \frac{\vec{p}(\vec{p}\vec{r})}{p^2} \right| \tag{2}$$

Here b can be calculated with respect to the beam-line or to the previously determined primary vertex.

2.1 Cuts

A neutral mother particle can be formed only if the two tracks have opposite electric charge. If there are n reconstructed tracks in an event, the number of such pairs can be estimated with $(n/2)^2$. For high multiplicity events the number of combinations is enormous. Therefore it is important to properly filter tracks and track-pairs in order to speed up the computation and to reduce the background. The distances available for cuts are summarized in Table 2.

Track level. The distribution of the the impact parameter of the positive and negative daughters are shown in Fig. 4 and Fig. 5, respectively. The background distribution is usually much narrower than that of the signal, because it consists of primary particles which have small impact parameter. There is one exception: protons from Λ decay (and antiprotons from $\overline{\Lambda}$) show a narrow peak. In this case the proton takes most of the Λ momentum and it seems as if it were a primary particle. The distributions are symmetric for V0s, while there are almost exclusively positive values for photons. The difference is due to the small q value of the photon conversion leading to a specific geometrical pattern.

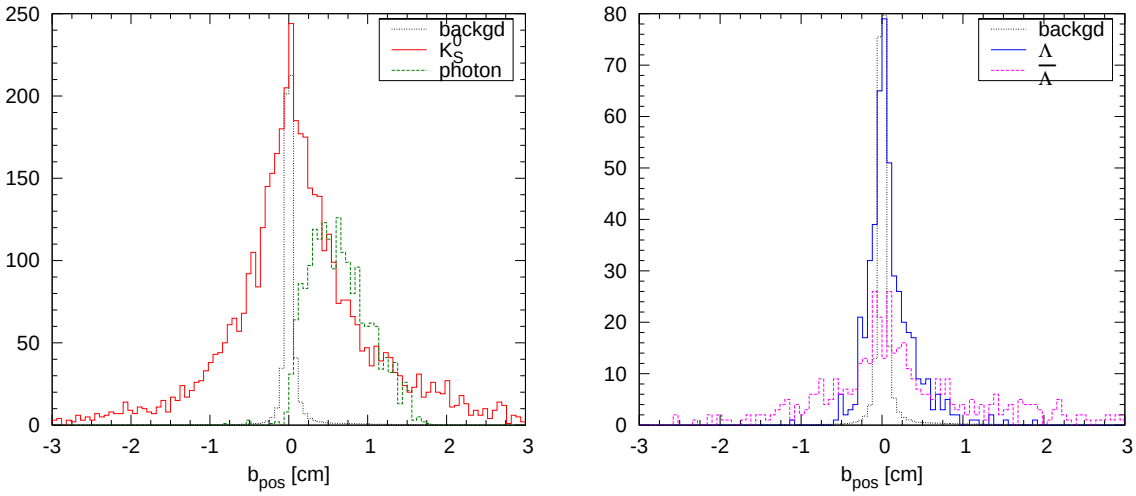

Figure 4: Distribution of the impact parameter of the positive daughters, shown for π^+ from K^0_S, e^+ from γ (left) and for p from Λ, π^+ from $\overline{\Lambda}$ (right). The rescaled background is indicated as well.

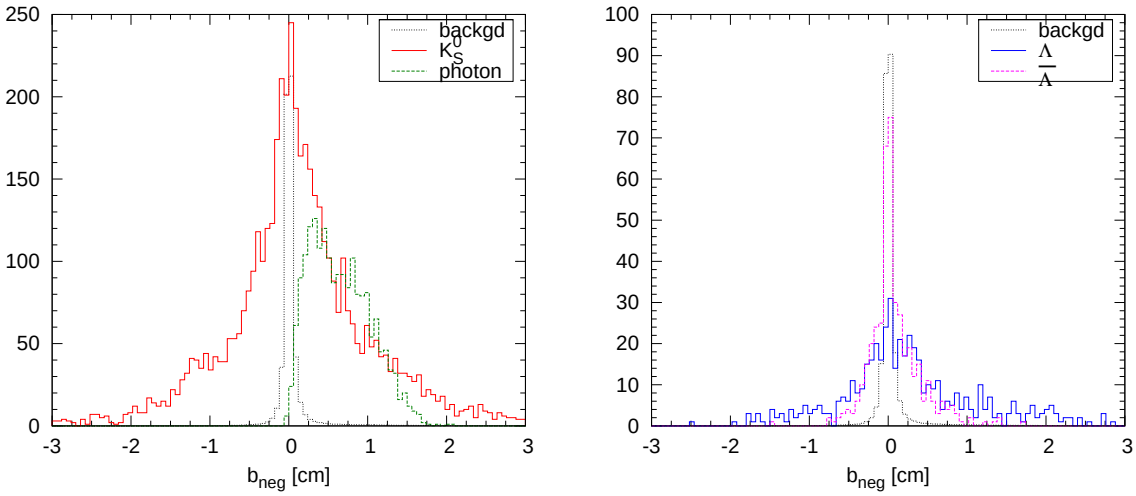

Figure 5: Distribution of the impact parameter of the negative daughters, shown for π^- from K^0_S, e^- from γ (left) and for $\overline{\mathrm{p}}$ from Λ, π^- from $\overline{\Lambda}$ (right). The rescaled background is indicated as well.

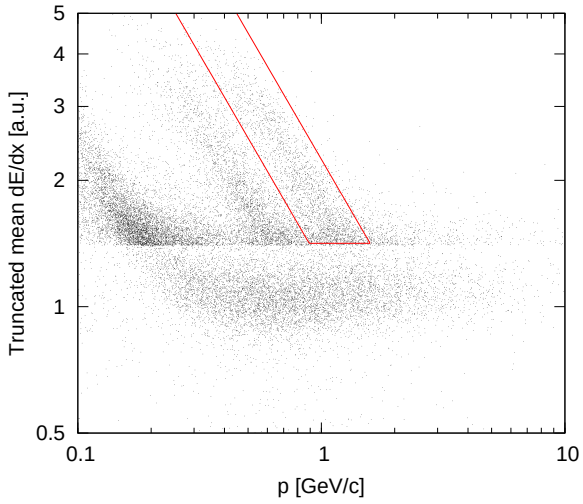

Figure 6: The truncated mean $\mathrm{d}E/\mathrm{d}x$ as function of total momentum p. Entries below the truncated mean value of 1.4 (arbitrary units) are suppressed by factor 10. The separation cut that encloses the protons is shown with the solid red lines.

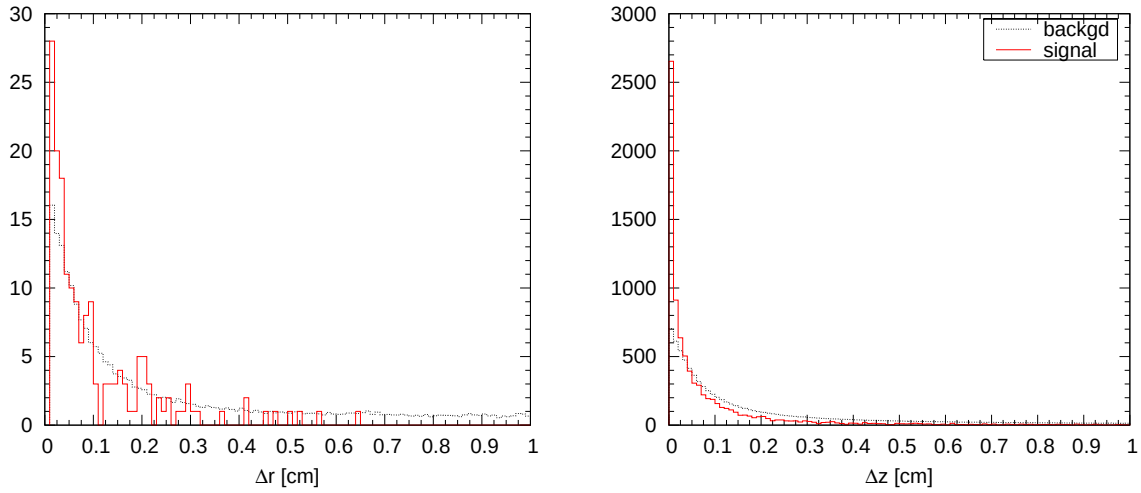

Figure 7: Distribution of the distance Δr of the projected circles of the daughters (left) and the distance Δz of closest points in z (right). The huge peak at $\Delta r = 0$ was suppressed. The background rescaled to the same area is indicated as well.

The impact parameters can be used to reduce background, a cut at 0.2 cm is reasonable. This can be applied to both positive and negative daughters from K^0_S and photons. In case of Λ only the pion can be cut for the reasons discussed in the previous paragraph which leads to high proton background. Although one cannot get rid of the primary protons, there is another way for the reduction of Λ background. In an event most of the produced particles are pions. The use of specific energy loss information in the pixel detector enables the clean selection of protons. The energy loss of the particles, in this case the easily calculable truncated mean $\mathrm{d}E/\mathrm{d}x$ is obtained as follows. The ADC values of the each pixel clusters are summed. The sum is divided by the path of the track inside the silicon. In the end there are three values corresponding to the three hits. They are ordered in increasing order $\Delta E/\Delta x_1 < \Delta E/\Delta x_2 < \Delta E/\Delta x_3$ and truncated by taking the average of the lower "half" of the numbers (50% truncation), that is $\mathrm{d}E/\mathrm{d}x = (\Delta E/\Delta x_1 + 0.5\Delta E/\Delta x_2)/1.5$. The resulted $\mathrm{d}E/\mathrm{d}x$ value as function of total momentum is shown in Fig. 6. With help of a separation cut the protons can be identified below 1.5 GeV/c and with good efficiency below 1 GeV/c.

Track-pair level. The distributions of distances Δr and Δz from the closest point calculation are shown in Fig. 7. Here the signal distributions are significantly narrower, a cut at 0.2 cm reduces the background. This way the closest points are indeed required to be close in both transverse and longitudinal coordinates.

The distribution of the distance of the production vertex from the beam-line (r) and from the pre-determined primary vertex (d) are given in Fig. 8. The r and d distributions for V0s show an exponential behaviour which is steeper for K^0_S than for Λ, because the $c\tau$ value of the former is smaller. The r distribution for photons is completely different. There are two peaks at $r \approx 4$ cm and at $r \approx 4.7$ cm belonging to conversions in the inner

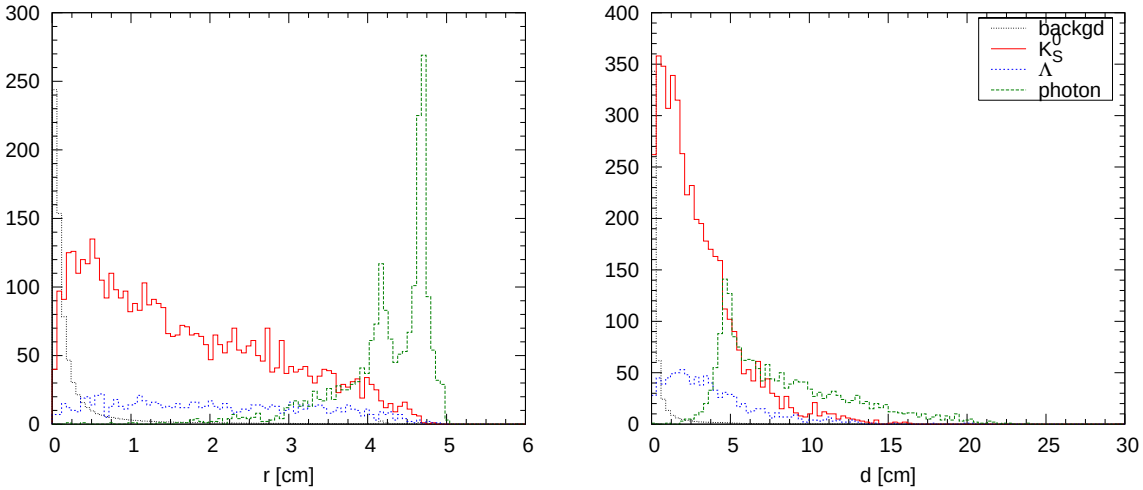

Figure 8: Distribution of the distance of the production vertex from the beam-line (r, left) and from the predetermined primary vertex (d, right). Histograms are shown for K^0_S, Λ and photon separately. The position of the inner and outer silicon wafers of the first pixel barrel layer are clearly visible in the r distribution of photons. The rescaled background is indicated as well.

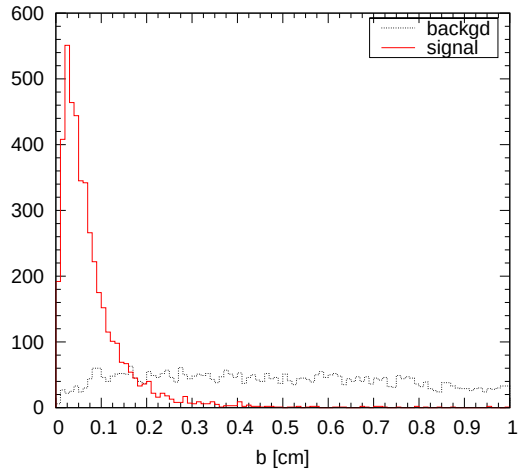

Figure 9: Distribution of the impact parameter of the mother particle with respect to the primary vertex. Histograms belonging to the background and signal are shown as well.

and outer silicon wafers of the first pixel barrel layer. (The conversions in the beam-pipe are hardly visible.) The background distribution peaks near zero as expected, a cut at 0.5 cm erases big part of the background.

The distribution of the impact parameter of the mother particle with respect to the beam-line or the primary vertex is shown in Fig. 9. The signal distribution is narrow, thus a cut at 0.2 cm takes out sizeable fraction of the background.

3 Results

Combined acceptance and efficiency of V0 and photon conversion reconstruction is shown in Fig 10. In the plateau region of $|\eta| < 1.5$ about 30% of the produced K^0_S, 20% of Λ and $\overline{\Lambda}$ are reconstructed. In case of photons the situation is worse, because they mostly come from π^0 decay and have low p_T.

3.1 Podolanski-Armenteros variables

The momenta of the daughters $\vec{p_1}$ and $\vec{p_2}$ can be decomposed to components parallel and perpendicular to the momentum of the mother particle $\vec{p} = \vec{p_1} + \vec{p_2}$. The longitudinal ones are obtained by

$$p_{1L} = \frac{\vec{p}\vec{p_1}}{p} \qquad\qquad p_{2L} = \frac{\vec{p}\vec{p_2}}{p} \tag{3}$$

The variables q_T and α are defined by

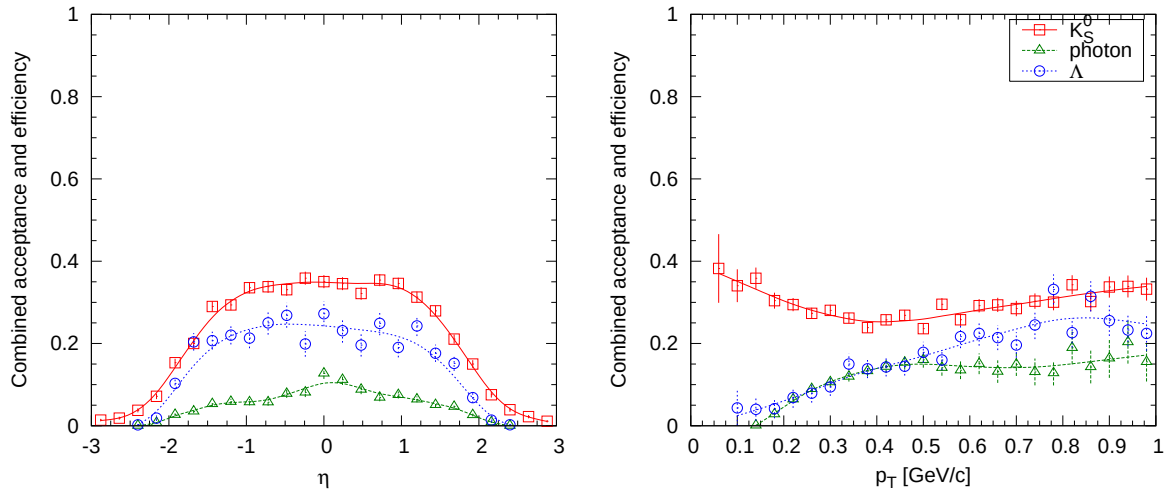

Figure 10: Combined acceptance and efficiency of V0 and photon conversion reconstruction (the ratio of the number of reconstructed to decayed or converted particles) as a function of η (left) and as a function of p_T (right, if the particle is in the range $|\eta| < 1$). Values for K^0_S, photon and Λ are shown separately.

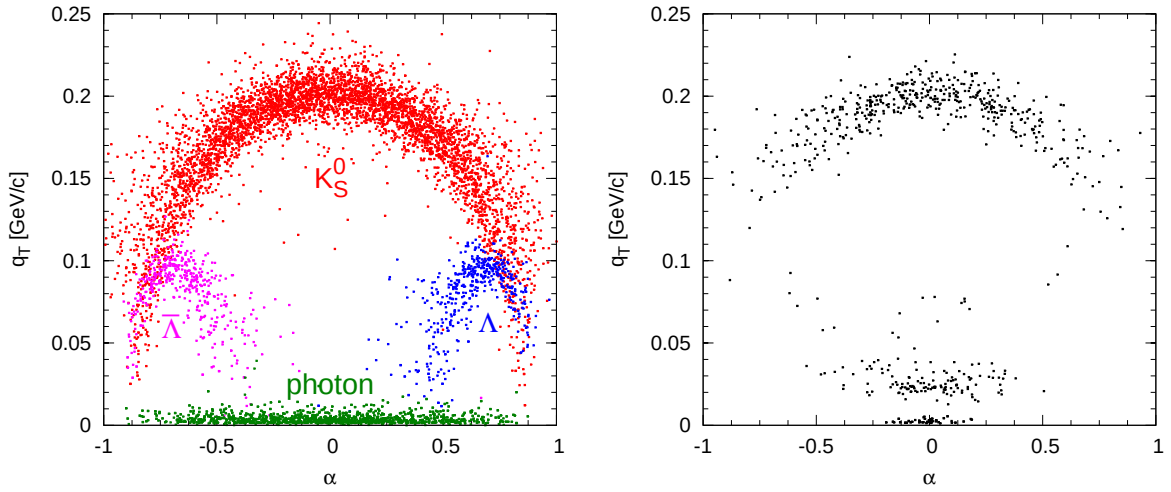

Figure 11: Armenteros plots. Simulated signal is shown on the left, where the position of K^0_S, Λ, $\overline{\Lambda}$ and photon is indicated. The result of the reconstruction with all the cuts applied is given on the right.

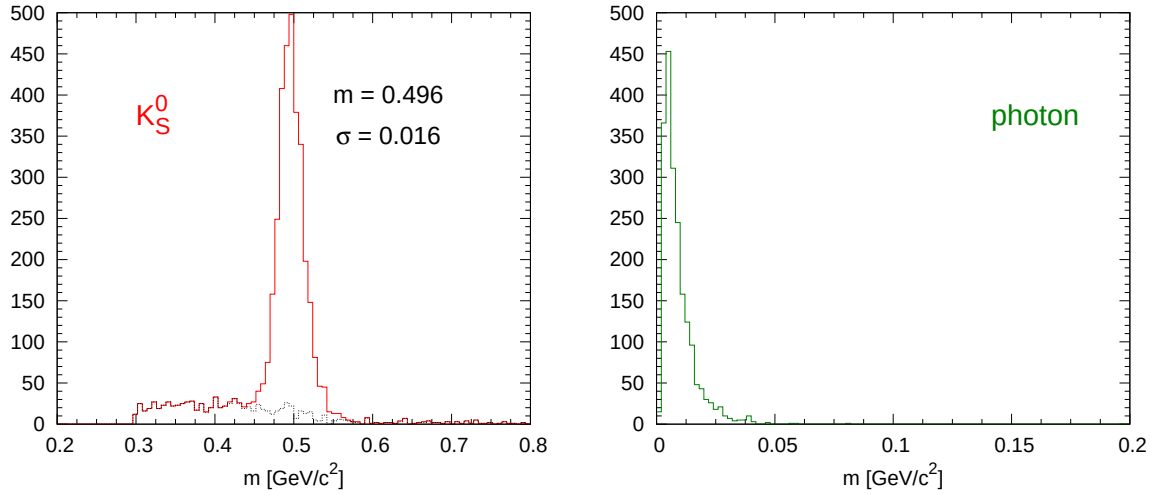

Figure 12: Invariant mass distribution of reconstructed K^0_S particles (left) and photons (right). In case of K^0_S the mass distribution of background is indicated as well (black dashed) and the result of the Gaussian fit is given in units of GeV/c^2.

$$q_T = \frac{|\vec{p_1} \times \vec{p_2}|}{p} \qquad \alpha = \frac{p_{1L} - p_{2L}}{p_{1L} + p_{2L}} = \frac{p_1^2 - p_2^2}{p^2} \tag{4}$$

For a given mother particle with mass m and momentum p that decays to particles with masses m_1 and m_2 the point pairs (α, q_T) lie on an ellipse [3]. The center of the ellipse is at $([m_1^2 - m_2^2]/m^2, 0)$. The half of the axis in q_T direction is the decay momentum q, while the half of the axis in α direction is $2q/(\beta m)$. Note that the latter depends on the momentum of the mother particle via β, lower momentum leads to wider ellipse. The Armenteros plots using simulated and reconstructed information are shown in Fig. 11. The Λs and $\overline{\Lambda}$s are suppressed because impact parameter cuts on both daughters are used.

The following cuts are used to separate or to enhance the particles: $q_T > 0.05$ GeV/c for K^0_S; $q_T < 0.02$ GeV/c for photon; $0.01 < q_T < 0.12$ GeV/c for Λ and $\overline{\Lambda}$.

3.2 Mass spectra

Invariant mass distributions of reconstructed particles are shown in Fig. 12 and Fig. 13. The importance of the $\mathrm{d}E/\mathrm{d}x$ selection for the secondary proton or antiproton is well visible, the cut removes almost all the background. The K^0_S is reconstructed with the resolution of 16 MeV/c^2 and at an average mass of 0.496 GeV/c^2. This agrees with the nominal mass value. At the same time Λ and $\overline{\Lambda}$ have a resolution of 6 MeV/c^2 and they are located at 1.114 GeV/c^2.

3.3 Performance at various conditions

The performance of V0 and photon conversion reconstruction was studied under several running conditions.

- Minimum bias p+p events with pile-up

  These studies are based on 25 000 minimum bias p+p events (Pythia generator). The events have been grouped according to Poissonian distribution in order to study the effect of pile-up at low-luminosity ($2 \cdot 10^{33}\mathrm{cm}^{-2}\mathrm{s}^{-1}$, 5 events per bunch-crossing on average) and at high-luminosity ($10^{34}\mathrm{cm}^{-2}\mathrm{s}^{-1}$, 25 events per bunch-crossing on average). Only in-time pile-up was considered.

Invariant mass distributions of the reconstructed K^0_S and Λ are shown in Fig. 14. The histograms of pile-up events have been normalized such that they correspond to the same number of produced particles as in the single p+p case. In case of single collisions and low-luminosity pile-up the resonances can be exclusively identified. For high-luminosity the inclusive yield can still be extracted with reasonable background. The same is true for Pb+Pb collisions (plot not shown in this note).

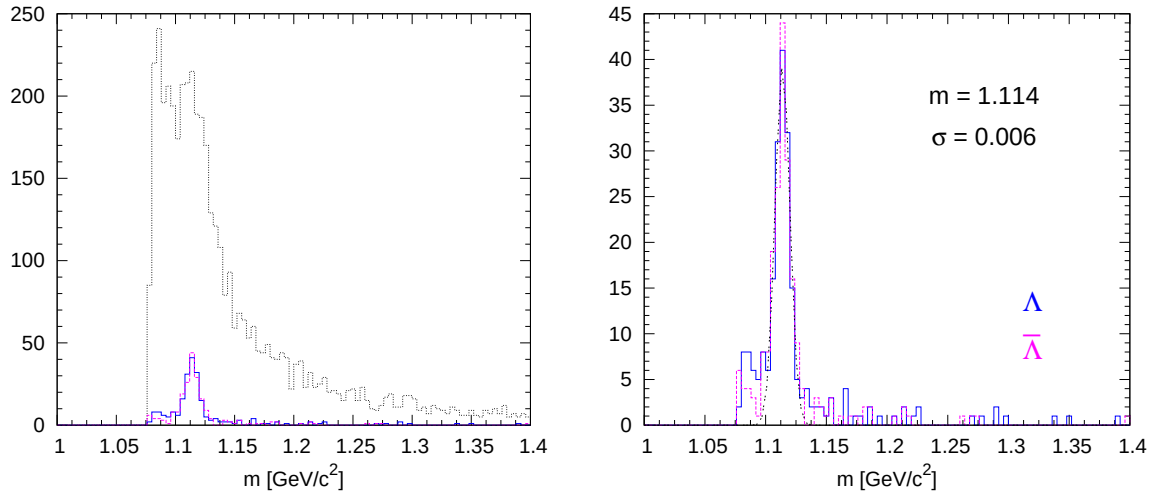

Figure 13: Invariant mass distribution of reconstructed Λ and $\overline{\Lambda}$ particles. The distribution without $\mathrm{d}E/\mathrm{d}x$ selection for the secondary proton or antiproton is shown on the left (dotted black). The solid histograms give the final result with $\mathrm{d}E/\mathrm{d}x$ selection switched on. They are re-plotted on the right with adjusted vertical scale. The result of the Gaussian fit is given in units of GeV/c^2.

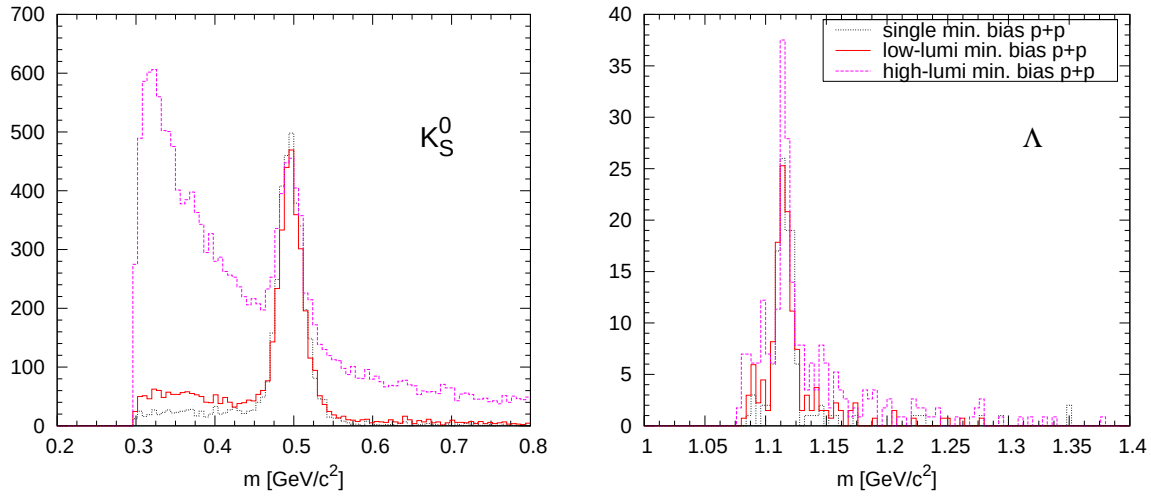

Figure 14: Invariant mass distribution of reconstructed K^0_S (left) and Λ (right) using single, low-luminosity and high-luminosity minimum bias p+p events.

4 Further developments

The cuts have been chosen by trial and error. Better performance can be achieved with neural network optimisation. The method presented in this note is usable not only for pixel tracks but to global tracks as well, as long as they have a well defined set of parameters at the perigee.

There are other V0-like objects which can be found with slight modification of the method described in this note: loopers and vertices of inelastic interactions. A looping particle in a turn leaves two hit triplets in the pixel detector. They are reconstructed as two separate tracks, one of them positively and the other one negatively charged. Secondary particles from an inelastic interaction show a pattern similar to V0s, but with two differences. The vertex can have more than two daughters ("star") which can be of both charges. Furthermore, the summed momentum of two secondaries does not necessarily point to the primary vertex.

If the impact parameter cut is relaxed, the found Λs can be used for the reconstruction of other weakly-decaying barions. By adding a π^- the doubly strange Ξ^- can be extracted which decays via $\Xi^- \rightarrow \Lambda\pi^-$ with 100% branching. The combination with a K^- gives the triple strange Ω^- which decays via $\Omega^- \rightarrow \Lambda\mathrm{K}^-$ with 67.8% branching. The V0 finding in this case simplifies to the search for the closest approach of the line of the Λ and the helix of the π^- or K^-.

5 Conclusions

Although neutral particles do not create hits in the pixel detector, they can be observed via their charged daughters. The combination of helices of secondaries enables the reconstruction of low p_T weakly-decaying particles (K^0_S, Λ and $\overline{\Lambda}$) decaying before the first pixel barrel. Low p_T photons converting in the beam-pipe or in the first pixel barrel are detectable as well. The observed mass widths of 6 MeV/c^2 and 15 MeV/c^2 are compatible with the resolution of momentum reconstruction.

Acknowledgement

The author wishes to thank to Gergely Patay, Pascal Vanlaer, Dániel Barna and other members of the Heavy Ions, Tracker/b-τ and MB/UE groups for helpful discussions. This work was supported by the Hungarian Scientific Research Fund (T 048898).

References

[1] J. P. Revol [ALICE Collaboration], *"Low-P_T Proton-Proton Physics at Low Luminosity at LHC"*, Eur. Phys. J. directC **4S1** (2002) 14 [Pramana **60** (2003) 795].

[2] Ferenc Siklér, *"Reconstruction of low p_T charged particles with the pixel detector"*, **CMS Note AN-2006/100**.

[3] J. Podolanski and R. Armenteros, Phil. Mag. **45** (1954) 13.

A Closest point(s) of two helices

If there are many selected tracks it is important to find the closest point of the helices quickly. Here a fast straightforward method is presented which can be used as a good starting point for further optimisation. It allows to make early decisions based on the distances that become available as the computation proceeds.

A reconstructed track can be parametrised at its closest approach to the beam-line, the perigee P by the following quantities:

- electric charge q
- transverse impact parameter b, signed by trajectory center C such that it is negative if the track circles around the beam-line, positive otherwise
- longitudinal position z of perigee P
- transverse momentum p_T

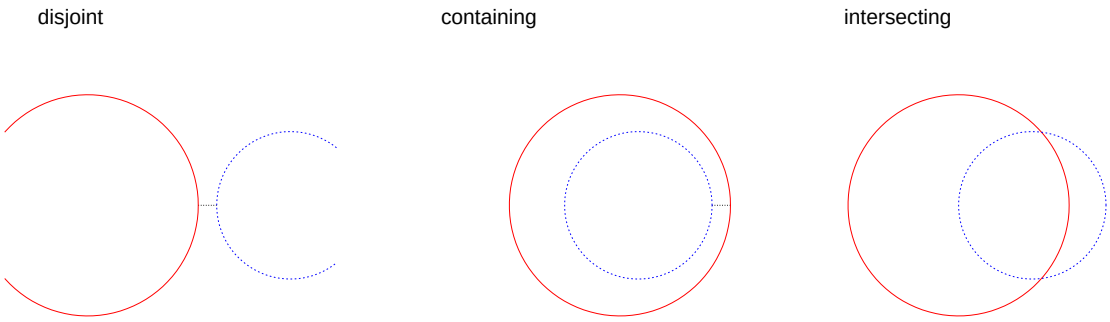

Figure 15: Possible relative placements of the projected circles: the circles are disjoint; one circle contains the other; the circles intersect in two points. The smallest distances are indicated in the first two cases.

- polar angle θ of the trajectory
- azimuthal angle ϕ, direction, of the trajectory

The geometrical objects are projected onto the transverse plane first. The image of the beam-line is the point O. A helix of a track is mapped to a circle with center C and radius $r = p_T/(0.003B)$, in units of cm, GeV/c and T, respectively. Note that $OP = |b|$ and $CP = r$. The direction of vector $\vec{CP}$ is given by the angle $\chi = \arg \vec{CP} = \phi + q\pi/2$. The coordinates of the center $C(x, y)$ are

$$x = -(r + b)\cos\chi \qquad\qquad y = -(r + b)\sin\chi \tag{5}$$

A helix pair gives two projected circles (C_1, r_1) and (C_2, r_2). The distance of the centers is $r_{12} = C_1C_2$. The direction of the vector $\vec{C_1C_2}$ pointing from the center of the first to that of the second circle is given by the angle $\psi = \arg \vec{C_1C_2}$. The azimuthal angles ψ_1, ψ_2 of the closest points and the smallest distance Δr can be calculated. Depending on the relative placement of the circles (Fig. 15) they will have a pair of closest points or two intersections:

1. The circles are disjoint ($r_{12} > r_1 + r_2$). The closest points and the smallest distance are

$$\psi_1 = \psi \qquad\qquad \psi_2 = \psi + \pi \qquad\qquad \Delta r = r_{12} - (r_1 + r_2) \tag{6}$$

2. One circle contains the other ($r_{12} < |r_1 - r_2|$). The closest points and the smallest distance are

$$\psi_1 = \psi_2 = \begin{cases} \psi & \text{if } r_1 > r_2 \\ \psi + \pi & \text{otherwise} \end{cases} \qquad\qquad \Delta r = |r_1 - r_2| - r_{12} \tag{7}$$

3. The circles intersect ($r_{12} < r_1 + r_2$ and $r_{12} > |r_1 - r_2|$). The smallest distance is $\Delta r = 0$. There are two intersections (index i) for each circle.

$$\gamma = \arccos\left(\frac{r_1^2 - r_2^2 + r_{12}^2}{2r_1r_{12}}\right) \tag{8}$$

$$\psi_{1,i} = \psi \pm \gamma \tag{9}$$

$$\psi_{2,i} = \arg(x_1 + r_1\cos\psi_{1,i} - x_2, y_1 + r_1\sin\psi_{1,i} - y_2) \tag{10}$$

Let V denote one of the closest points, its projection. The central angle is given by

$$\angle PCV = \Delta\psi = \psi - \chi + k2\pi \tag{11}$$

where k is an integer chosen such that $-\pi < \Delta\psi < \pi$. For a valid track $q\Delta\psi < 0$ must hold. The closest point can be mapped back to three dimensions onto one of the helices. The coordinates of V are thus given by

$$V(x + r\cos\psi, y + r\sin\psi, z - qr\cot\theta\Delta\psi) \tag{12}$$

There are two such points V_1 and V_2, belonging to the first and second helix, respectively. The distance of closest points in z direction is given by $\Delta z = |z_2 - z_1|$.

The production vertex can be approximated by the midpoint of the line segment V_1V_2. If the projected circles intersect there are two pairs of closest points. In this case the pair with smaller Δz value is chosen. The momentum components of a track at the vertex are obtained by

$$p_x = qp_T\sin\psi \qquad p_y = -qp_T\cos\psi \qquad p_z = p_T\cot\theta \tag{13}$$

B Event gallery

Plots of reconstructed V0s and photon conversions in single minimum bias p+p events are shown in Fig. 16.

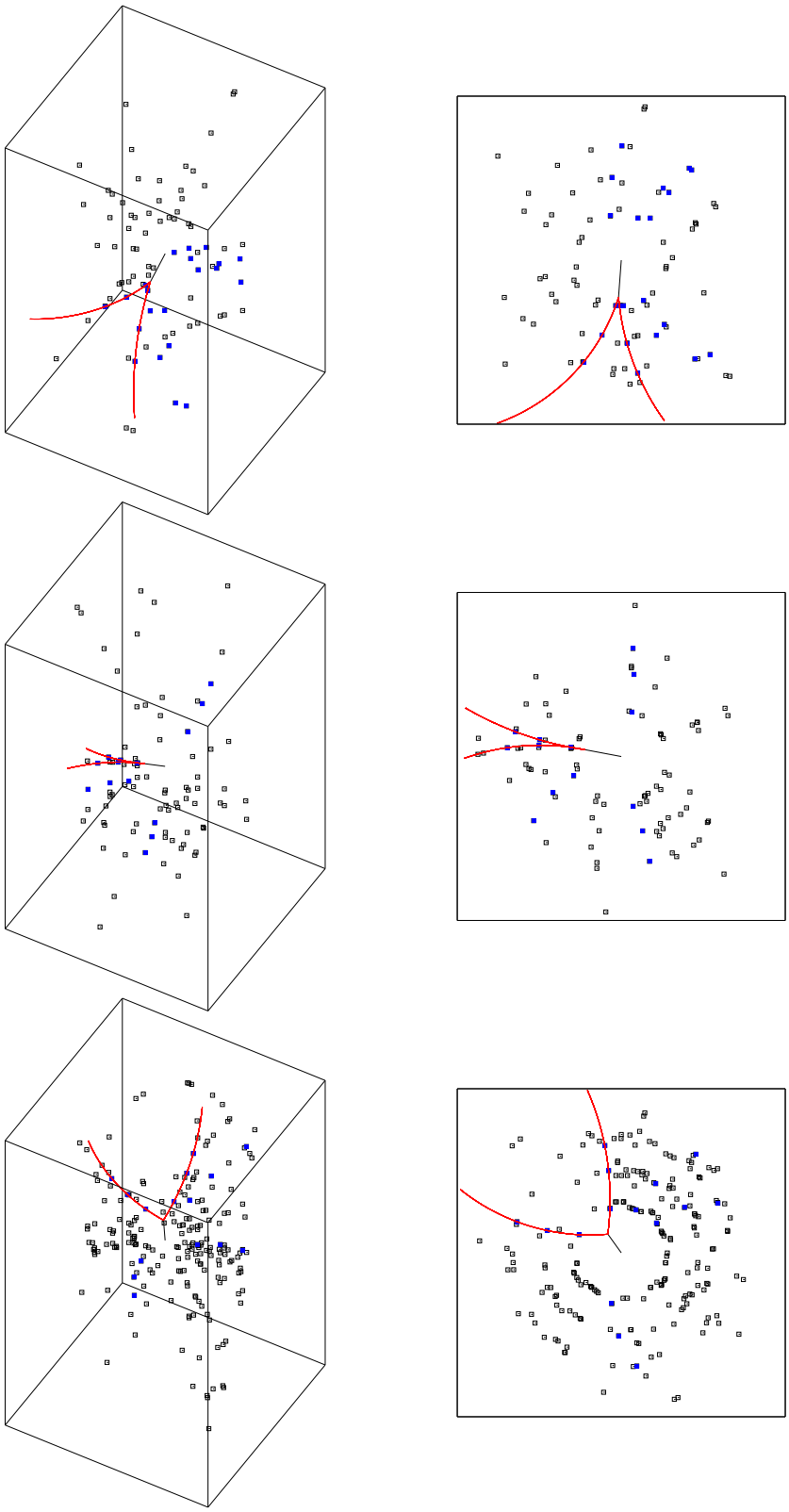

Figure 16: Plots of reconstructed V0s and photon conversions in single minimum bias p+p events. Hits are shown by open black boxes. Those hits which belong to a secondary reconstructed track are indicated by filled blue boxes. The helices of the reconstructed daughter trajectories are drawn with solid red lines. The path of the neutral mother particles are indicated by the thick black straight lines. Both the three dimensional view and its planar projection are shown.